Environmental Pollution 190 (2014) 166–175

Contents lists available at ScienceDirect

Environmental Pollution

journal homepage: www.elsevier.com/locate/envpol

# Source apportionment of atmospheric mercury pollution in China using the GEOS-Chem model

Long Wang [a,b], Shuxiao Wang [a,b,c,*], Lei Zhang [a,b], Yuxuan Wang [d,e], Yanxu Zhang [f], Chris Nielsen [f], Michael B. McElroy [f], Jiming Hao [a,b,c]

[a] State Key Joint Laboratory of Environment Simulation and Pollution Control, School of Environment, Tsinghua University, Beijing 100084, China
[b] Collaborative Innovation Center for Regional Environmental Quality, Tsinghua University, Beijing 100084, China
[c] State Environmental Protection Key Laboratory of Sources and Control of Air Pollution Complex, Beijing 100084, China
[d] Ministry of Education Key Laboratory for Earth System Modeling, Center for Earth System Science, Tsinghua University, Beijing 100084, China
[e] Department of Marine Sciences, Texas A&M University at Galveston, Galveston, TX 77553, USA
[f] School of Engineering and Applied Sciences, Harvard University, Cambridge MA 02138, USA

ARTICLE INFO

*Article history:*
Received 31 October 2013
Received in revised form
4 March 2014
Accepted 8 March 2014
Available online 23 April 2014

*Keywords:*
Nested-grid GEOS-Chem
Mercury pollution
Industrial sources
Control policy
China

ABSTRACT

China is the largest atmospheric mercury (Hg) emitter in the world. Its Hg emissions and environmental impacts need to be evaluated. In this study, China's Hg emission inventory is updated to 2007 and applied in the GEOS-Chem model to simulate the Hg concentrations and depositions in China. Results indicate that simulations agree well with observed background Hg concentrations. The anthropogenic sources contributed 35–50% of THg concentration and 50–70% of total deposition in polluted regions. Sensitivity analysis was performed to assess the impacts of mercury emissions from power plants, non-ferrous metal smelters and cement plants. It is found that power plants are the most important emission sources in the North China, the Yangtze River Delta (YRD) and the Pearl River Delta (PRD) while the contribution of non-ferrous metal smelters is most significant in the Southwest China. The impacts of cement plants are significant in the YRD, PRD and Central China.



## 1. Introduction

Mercury is toxic, persistent and bio-accumulative and can be transported over long distances. Atmospheric mercury exists mostly in inorganic forms in one of three states: GEM (gaseous elemental mercury, $Hg^0$), RGM (reactive gaseous mercury in divalent form, $Hg^{2+}$) and PHg (particulate mercury). Different forms have different physical and chemical properties which can greatly influence the mercury transport, transformation and removal processes.

Mercury is emitted from both anthropogenic and natural sources. Anthropogenic emissions have largely enhanced the mercury cycle in the biosphere. China emitted 576 t mercury in the year 2010, accounting for about 35% of the global anthropogenic mercury emissions (AMAP/UNEP, 2013). Coal-fired power plants, non-ferrous smelters and cement plants are important sources in China and emit 97 t, 83 t (from lead, zinc, copper, large scale gold production) and 85t respectively. Previous observations have shown that China is suffering from heavy pollution of atmospheric mercury. High Hg concentrations are not only reported in cities (Fang et al., 2004; Liu et al., 2011; Wang et al., 2007) but also at some rural and remote sites (Ci et al., 2011a; Fu et al., 2010a,b; Wan et al., 2009a). In cities and rural areas the reported TGM concentrations are in the ranges 5–18 ng $m^{-3}$ and 2.5–6 ng $m^{-3}$, respectively, which are much higher than the background value of 1.5–1.7 ng $m^{-3}$ in the northern hemisphere (Slemr et al., 2011, 2003).

Observations can only inform the levels of mercury pollution in a specific region, while models such as CMAQ-Hg, GEOS-Chem, STEM-Hg can help us to understand the spatial and temporal distribution of mercury concentrations and deposition over a large scale, and in particular, to identify the contributions of emission from different sources. These models are different from each other in the fundamental assumptions regarding chemical reactions, deposition and transport of mercury in the atmosphere. Model evaluation using observations such as American Mercury Deposition Network (MDN) datasets and model inter-comparison were conducted (Bullock et al., 2008, 2009; Ryaboshapko et al., 2007a,b) to narrow this gap. The evaluation indicated that the models can be used in a global or regional scale over a relatively long period. The GEOS-Chem mercury model in a global scale with a horizontal

* Corresponding author.
*E-mail address:* shxwang@tsinghua.edu.cn (S. Wang).

http://dx.doi.org/10.1016/j.envpol.2014.03.011
0269-7491/

resolution of 4° × 5° has been verified by Selin et al. (2007) and updated by Holmes et al. (2010). The model reproduced the annual mean total gaseous mercury (TGM) observations from 22 land-based sites and predicted the magnitude of wet deposition within 10% nationally. CMAQ-Hg model is a regional Eulerian model first implemented by Bullock and Brehme (2002). Analysis of the uncertainties of key physical and chemical parameters in this model was performed by Lin et al. (2006), Lin et al. (2007) and Pongprueksa et al. (2008). The simulated mercury concentrations correlated well with measurements and diurnal and seasonal pattern can also be reproduced in the Canadian Atmospheric Hg Measurement Network (CAMNet) monitoring stations (Gbor et al., 2006).

These models were used for the analysis of regional mercury pollution and its long-range transport. The GEOS-Chem model was used for analysis of spatial and seasonal patterns of mercury wet deposition in America and the dominant factors for the variations for different seasons in different regions were located (Selin and Jacob, 2008). The trans-Pacific transport of mercury was also estimated by GEOS-Chem model with observations from four typical sites along the pathway (Strode et al., 2008). The results showed Asia anthropogenic sources contributed 14% to deposition in North America. CMAQ-Hg (Lin et al., 2010), and STEM-Hg (Pan et al., 2010) were used to study the mercury pollution in China and the mercury budget in East Asia. Model evaluation show the models can capture the chemistry of mercury. Pan et al. (2010) estimated the annual mean GEM, RGM and PHg is 1.8 ng $m^{-3}$, 100 pg $m^{-3}$ and 150 pg $m^{-3}$, respectively and the mercury outflow caused by anthropogenic sources was estimated to be 681–714 t $yr^{-1}$ in 2001. Lin et al. (2010) estimated the outflow of mercury caused by emission in East Asia to be in the range of 1396–1671 t $yr^{-1}$ by CMAQ-Hg, of which 50–60% was caused by natural sources. Wang et al. (2013) used Regional Atmospheric Environment Model (RegAEMs) to simulate atmospheric mercury and found the Hg concentration in most areas of China exceed the global background level of 1.0 ng $m^{-3}$ except those in West and Northwest China.

In this paper, we use the GEOS-Chem model to simulate mercury chemical transport in the nested East Asia domain in 2009. Available monitoring data were used to evaluate the model performance with baseline emission scenario. The impacts of mercury emissions from typical industrial sources including power plants, non-ferrous metal smelters and cement plants on the whole China domain and developed regions such as the North China (NC) and the Yangtze River Delta (YRD) are quantified through sensitivity analysis. The results can help policy-makers establish control measures in a more effective way.

## 2. Methodology

### 2.1. Model description

The GEOS-Chem model is a global 3-D model of atmospheric chemistry and transport driven by assimilated meteorological data from the Goddard Earth Observing System (GEOS) of the NASA Global Modeling and Data Assimilation Office

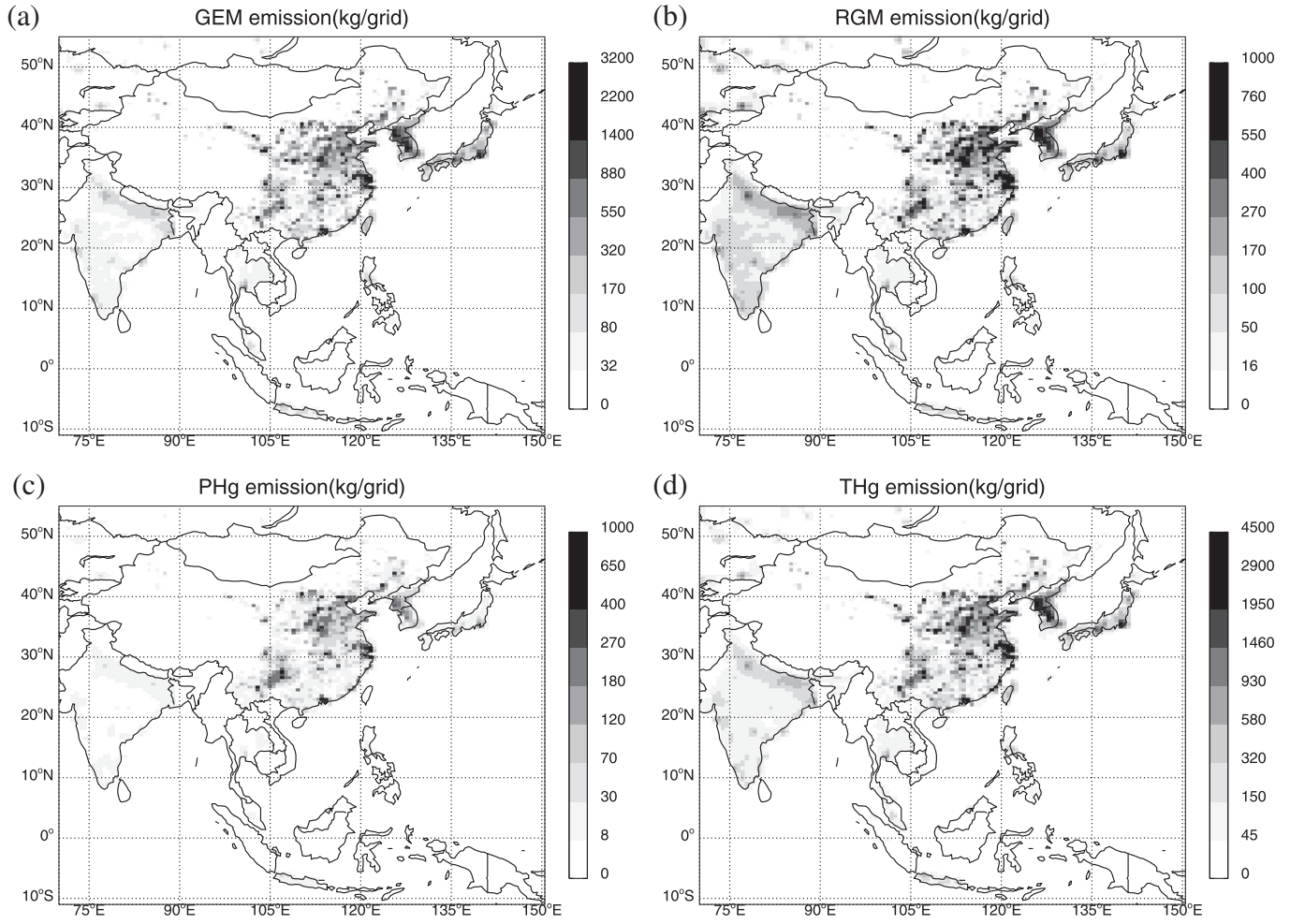


**Fig. 1.** Spatial distribution of anthropogenic mercury emission in the study domain, kg $grid^{-1}$ $yr^{-1}$. (a) Gaseous elemental mercury (GEM); (b) Reactive gaseous mercury (RGM); (c) Particulate mercury (PHg); (d) Total mercury (THg).

(GMAO). The Hg simulation in the GEOS-Chem model was first described and evaluated by Selin et al. (2007). In this model, GEM is oxidized to RGM in the gaseous phase in the presence of OH, $O_3$ and Br. In-cloud (aqueous) photochemical reduction of RGM to GEM is included with a reduction rate relating to the photolysis rate of $NO_2$. PHg is considered chemically inert and can only be removed by dry and wet deposition. Mercury emission from natural sources like vegetation, soil, ocean and snow are estimated online and mercury re-emission is also considered. In the model, 20% of RGM and PHg deposition in the terrestrial system is re-emitted as $Hg^0$ simultaneously while 60% is re-emitted from snow surface (Holmes et al., 2010).

In this study, the nested-grid GEOS-Chem model is used over East Asia domain (11°S–55°N, 70°E–150°E) consisting of 121 × 133 horizontal grids with a spatial resolution 0.5° × 0.667° (about 40 km × 50 km in China) and 47 vertical layers from the surface to about 80 km altitude. The nested-grid capability in the GEOS-Chem global model was first developed by Wang et al. (2004) and extended to the GEOS-5 meteorology by Chen et al. (2009). The nested-grid Hg simulation was developed by Zhang et al. (2012) for the North American domain and we adopted here for the nested-grid East Asia domain. The input datasets such as Br concentration fields, natural primary production (NPP) and the upwelling velocity from Ekman pumping for East Asia were regridded from global 4° × 5° or 2° × 2.5° data. The global GEOS-Chem model with a resolution of 4° × 5° was run for the period 2006–2009 to provide the initial and boundary conditions and the simulation period for East Asia was January to December, 2009.

### 2.2. Emission inventory and scenarios

In this study, the mercury emission inventory in China was updated to 2007 using a methodology similar to that proposed by Wu et al. (2006) while methodologies for power plants and non-ferrous smelters were updated using recent studies (Wang et al., 2010a,b,c). For estimation of mercury emission from power plants, we considered coal produced in different provinces, a new coal transport matrix, mercury content in coal consumed, release ratio of mercury in different boiler types and the removal efficiencies and speciations of different combinations of atmosphere pollution control devices (APCDs). For non-ferrous smelters, we used the methodology based on mass balance of mercury in smelting processes (Wu et al., 2012) to estimate emission factors in provincial level, other than national fixed emission factor used by Streets et al. (2005), Wu et al. (2006) and AMAP/UNEP (2013). Mercury content in zinc/lead/copper ore concentrate produced and consumed, and installations and removal efficiencies of various APCDs such as dust collectors (DC) were considered in this study.

In 2007, mercury emission from anthropogenic sources in China was 643.1 t, of which 49.4% was GEM, 38.4% was RGM and 12.2% was PHg. The emissions were mainly from coal combustion (57.3%) and non-ferrous metal smelting (18.2%). Cement production, iron/steel production and waste incineration were also important sources which released 88.0 t (13.6%), 19.6 t (3.0%) and 20.0 t (3.1%) respectively. Emission inventories outside China (totally 311.8t) in the study domain were based on the work by Streets et al. (2009). Fig. 1 shows the spatial distribution of GEM, RGM and PHg emissions in the study domain. All power plants were treated as large point sources and the distribution of emissions from other sources were based on the methodology given in Fu et al. (2013).

Five scenarios were established to study the effects of typical industrial sources. First, we run the base scenario denoted as "BASE" with the mercury inventory in 2007, and the scenario named "NAT" with only natural emissions to see the effects of total anthropogenic emissions. Then, we set emissions from coal-fired power plants, non-ferrous smelters and cement kilns to zero one by one for simulation. These three scenarios were named as "NOPP", "NONF" and "NOCE", respectively. Fig. 2 shows emissions of mercury from the three sectors in China.

We selected six domains for analysis as shown in Fig. 3: the North China (NC; 33°45′N–42°15′N, 107°40′E–119°E), the Yangtze River Delta (YRD, 28°45′N–32°45′N, 117°40′E–122°20′E), the Central China (CC, 26°45′N–32°45′N, 109°40′E–116°20′E), the Pearl River Delta (PRD, 21°15′N–24°45′N, 111°E–115°40′E), the Southwest China (SWC; 24°15′N–31°45′N, 102°20′E–107°40′E) and CHINA (18°15′N–53°45′N, 73°E–135°E). The CHINA domain covers the entire Chinese Mainland and the THg concentrations of the other five domains are 35–50% larger than that of the CHINA domain. For all grids in a domain, we calculated the mean TGM concentration, along with the mean dry and wet deposition in different scenarios, and then compared these results to see the environmental effects of these sources.

### 2.3. Model evaluation

Observations at 16 rural or remote sites, of which 2 were shipboard and others were land-based were used to evaluate the model performance. The locations of these sites are shown in Fig. 3. Mt. Waliguan and Mt. Leigong, two inland sites which are not influenced by local sources through horizontal convection due to their higher elevations than nearby industrial cities, represent the background mercury levels in Chinese Mainland. Okinawa, an island along the East China Sea, far from anthropogenic activities, can reflect the mercury concentrations in marine boundary layer in East Asia. Comparisons with observations from cities were not included because these observations may not well represent mean mercury concentrations of the grid cell where they locate because emissions are instantaneously diluted in grid cells in the GEOS-Chem.

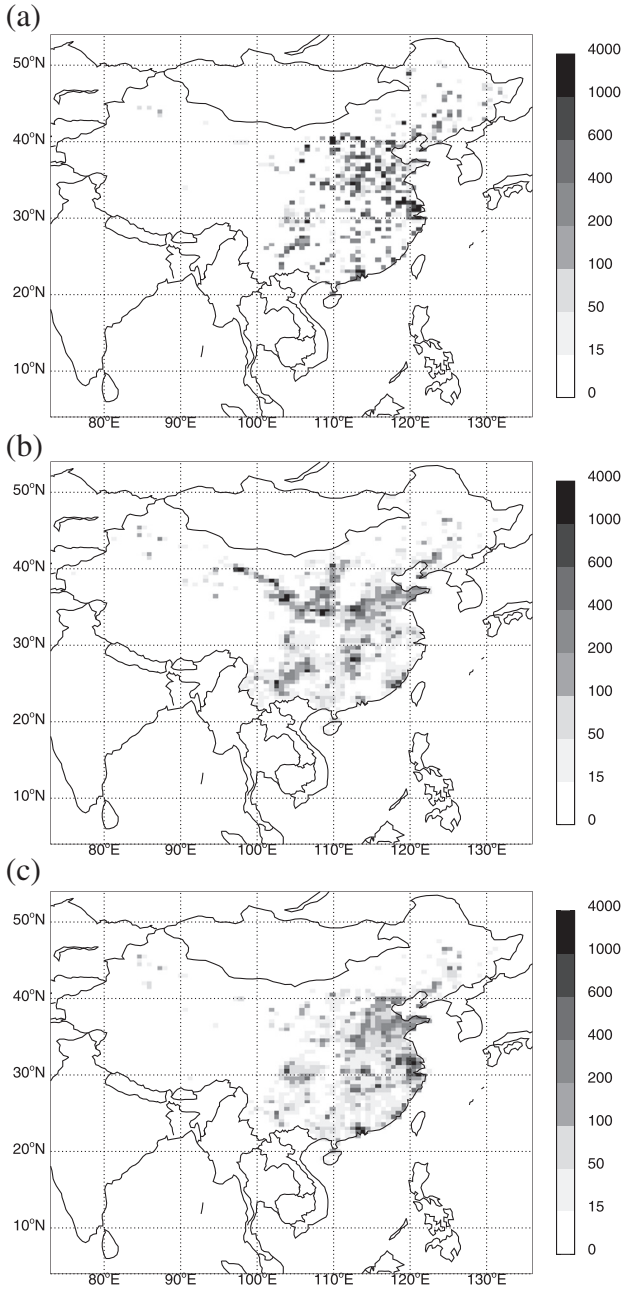


**Fig. 2.** Spatial distribution of total mercury emission from typical sectors, kg grid$^{-1}$ yr$^{-1}$. (a) Power plants; (b) Non-ferrous smelters; (c) Cement Plants.

Monthly averages of TGM or GEM from Miyun, Mt. Leigong and Chongming were also compared with model simulations. Miyun is a rural site about 100 km northeast of the center of Beijing. Mt. Leigong is a rural site at the peak in Southwest China (Fu et al., 2010a). Chongming Island is about 80 km from the center of Shanghai and only 5 km to the East Sea. These sites can represent the background mercury levels in the NC, YRD and SWC respectively.

## 3. Results and discussion

### 3.1. Model results and evaluation

The annual average concentrations in surface air predicted by the model are shown in Fig. 4. The predicted concentrations of GEM, RGM and PHg were typically in the ranges of 1.3–2.0 ng m$^{-3}$, 5–80 pg m$^{-3}$ and 6–100 pg m$^{-3}$, while the maximum reached

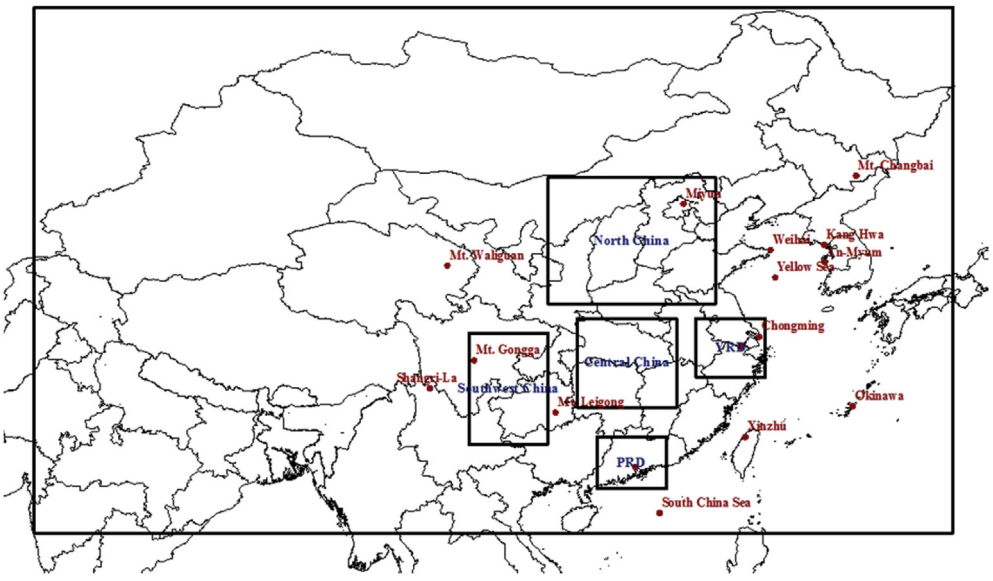


**Fig. 3.** Locations of mercury monitoring sites and the regions selected for comparison in sensitivity analysis.

4.5 ng $m^{-3}$, 817 pg $m^{-3}$, and 1790 pg $m^{-3}$, respectively. The GEM values are quite consistent with the previous global and regional model results (Lin et al., 2010; Pan et al., 2010). Much higher mercury concentrations are modeled over East China and Korea than neighboring areas due to the higher emission intensity. The NC and the YRD are the most polluted areas. In the CC, YRD and SWC, the mercury concentrations are also elevated compared to background areas.

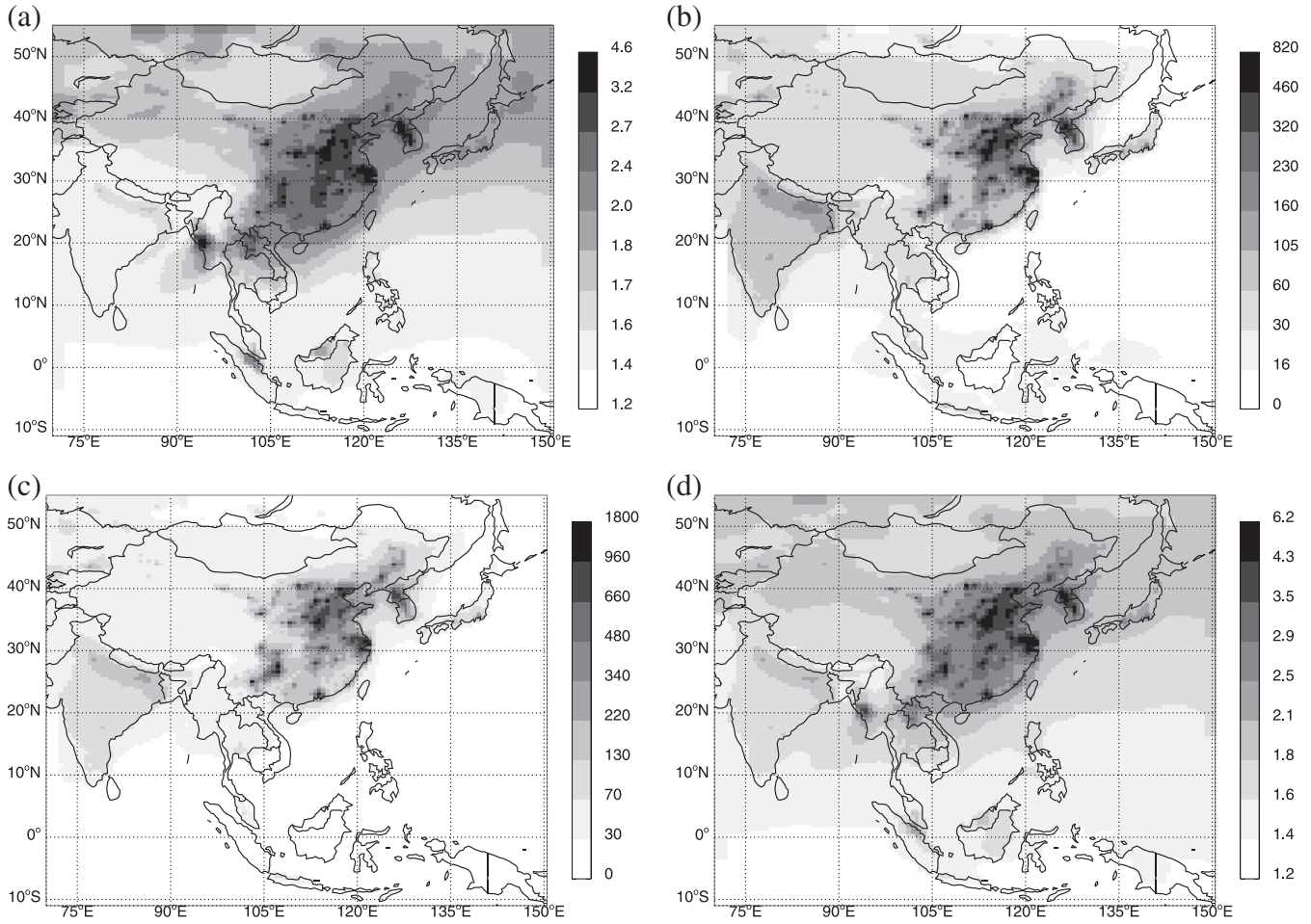


**Fig. 4.** Spatial distribution of mercury concentrations using Base scenario emissions. (a) Gaseous elemental mercury (GEM), ng $m^{-3}$; (b) Reactive gaseous mercury (RGM), pg $m^{-3}$; (c) Particulate mercury (PHg), pg $m^{-3}$; (d) Total mercury (THg), pg $m^{-3}$.

Table 1 lists the comparisons of model results with observations. In Mt. Waliguan, Mt. Leigong, and Okinawa, the modeled GEM is quite consistent with observations, with a bias no more than 10%. The consistency of model simulation and observation in background sites reflects that the model can simulate the main chemical and transport processes in this region. For the five rural sites including Chongming, Miyun, Mt. Gongga, Shang-ri and An-Myum which have monitoring data for at least a 1-year period, the model generally underestimates GEM or TGM. The model underestimates by about 45% at Mt. Gongga and An-Myum, about 35% in Shang-ri and about 25% in Chongming and Miyun. These sites may all be influenced by nearby cities within 100 km. The emissions can be well mixed in a regional scale in a normal meteorological condition, but enhanced Hg levels are observed when air mass arrived is from polluted areas and bad meteorological conditions emerge. The low model spatial resolution and the accuracy of emission allocation are two important reasons for the underestimate of TGM in these sites, and the underestimate of emission might be another. In both remote and rural sites, the model overestimates RGM and PHg by a factor of 2–5, which is the same as reported results by Zhang et al. (2012) in North America. This indicates possible overestimate of oxidation of GEM to RGM/PHg and the uncertainty of speciation of mercury emissions from anthropogenic sources or possible in-plume reduction of RGM to GEM in power plants or industrial boilers (Lohman et al., 2006).

Fig. 5a shows comparison of simulated and observed GEM concentrations from January to October in 2009 at Miyun Station. For GEM, the model reproduces the concentrations in winter, but underestimates it by about 40% from April to September. From the observation data, we can see that the GEM concentrations in summer are higher than that in winter. This may be due to the different dominant wind direction in the two seasons and natural sources may also play an important role (Zhang et al., 2013). The seasonal trend of model simulations is the reverse of the observations. One reason is that we may overestimate the deposition processes in the summer, and the other is that we underestimates the emissions in North China.

Fig. 5b shows the comparison of simulated and observed TGM at Mt. Leigong. The model can well predict the seasonal variations but the simulations are somewhat lower in summer and higher in winter. The observations signify the influence of the monsoon in Southwestern China. In summer, the southeast wind takes clean air mass from the sea, and in winter the wind takes air mass from the northeastern areas with high mercury emission intensities. The model does well in predicting mercury transport in the Southwestern China.

Fig. 5c shows the simulation and observation data of Chongming Station. The model can reliably predict the TGM from July to September, but underestimates TGM by a factor of 5 from October to December because it could not reproduce the heavy pollution events during the periods when the air masses came from North China. Fig. 5d shows modeled and observed average TGM concentrations from Sep 2009 to Dec 2009 in different wind directions. We can see modeled average TGM concentrations with air mass from the ocean (from 0 to 180°) are consistent with the observations. When wind was from west and northwest (292.5–337.5°), the model greatly underestimates TGM. This may be partly due to the low resolution of model grids and partly due to an underestimation of mercury emissions in the YRD and North China.

The spatial distributions of annually accumulated dry and wet deposition predicted by the model are shown in Fig. 6a. In the study domain, the dry and wet deposition range from 0 to 140 μg $m^{-2}$ $yr^{-1}$ and 0 to 200 μg $m^{-2}$ $yr^{-1}$ with an average of 12.3 μg $m^{-2}$ $yr^{-1}$ and 18.9 μg $m^{-2}$ $yr^{-1}$, respectively. In East China, the average annual dry deposition is over 35 μg $m^{-2}$ $yr^{-1}$. The wet deposition is obviously influenced by both precipitation and emissions. Southwest China with higher emission intensity and a large amount of rain precipitation shows high mercury wet deposition with an average more than 50 μg $m^{-2}$ $yr^{-1}$ and a peak value at about 200 μg $m^{-2}$ $yr^{-1}$.

**Table 1**
Comparisons of model results in BASE scenario with observations from remote and rural sites.

| Location | Sampling period | Observations | | | Model | | | Relative bias (TGM/GEM) % | Reference |
|---|---|---|---|---|---|---|---|---|---|
| | | TGM/GEM ng $m^{-3}$ | PHg pg $m^{-3}$ | RGM pg $m^{-3}$ | TGM/GEM ng $m^{-3}$ | PHg pg $m^{-3}$ | RGM pg $m^{-3}$ | | |
| Jiaxing, Zhejiang Province | Sep-05 | 5.4 | – | – | 4.3 | – | – | −20.4 | Wang et al. (2007) |
| Miyun, Beijing | Jan-09–Nov-09 | 3.2 | 98 | 8.9 | 2.4 | 465 | 238 | −25.0 | Zhang et al. (2013) |
| Chongming, Shanghai | Oct10–Jan-11, Feb-12–Apr-12 | 2.7 | 22 | 8 | 2.0 | 60 | 25 | −25.9 | Dou (2012) |
| Mt. Changbai, Jilin Province | Aug-05–Jul-06 | 3.6 | 65 | 77 | 1.9 | 86 | 60 | −47.2 | Wan et al. (2009a, 2009b) |
| | Oct-08–Oct-10 | 1.6 | – | – | 1.9 | – | – | 18.8 | Fu et al. (2012b) |
| Mt. Gongga, Sichuan Province | May-05–Apr-06 | 4 | 31 | 6.2 | 2.1 | 62 | 44 | −47.5 | Fu et al. (2008a, 2008b) |
| Mt. Leigong, Guizhou Province | May-08–May-09 | 2.8 | – | – | 2.8 | – | – | 0.0 | Fu et al. (2010c) |
| South China Sea | Aug-07 | 2.6 | – | – | 1.4 | – | – | −46.2 | Fu et al. (2010b) |
| Mt. Waliguan, Qinghai Province | Sep-07–Sep-08 | 2 | 19 | 7.4 | 1.8 | 36 | 34 | −10.0 | Fu et al. (2012a) |
| Chengshantou, Shandong Province | 2007–2009, four campaigns | 2.3 | – | – | 2.4 | – | – | 4.3 | Ci et al. (2011a) |
| Yellow Sea | Jul-10 | 2.6 | – | – | 2.1 | – | – | −19.2 | Ci et al. (2011b) |
| Wanqingsha, Guangdong Province | Dec-08 | 2.9 | – | – | 3.8 | – | – | 31.0 | Li et al. (2011) |
| Shangri-La, Yunnan Province | Nov-09–Nov-10 | 2.6 | 44 | 8.2 | 1.7 | 34 | 29 | −34.6 | Zhang (2011) |
| An-Myum, South Korea | Dec-04–Apr-06 | 4.6 | – | – | 2.5 | – | – | −45.7 | Nguyen et al. (2007) |
| Okinawa, Japan | Mar-04–May-04 | 2.0 | 4.5 | 3.0 | 1.9 | 16 | 11 | −5.0 | Chand et al. (2008) |
| Kang Hwa, South Korea | Mar-01 | 3.7 | – | – | 2.6 | – | – | −29.7 | Kim et al. (2002) |
| Xinzhu, Taiwan | Sep-03–Dec-03, Apr-04–Jun-04 | 6.1 | – | – | 2.0 | – | – | −67.2 | Kuo et al. (2006) |

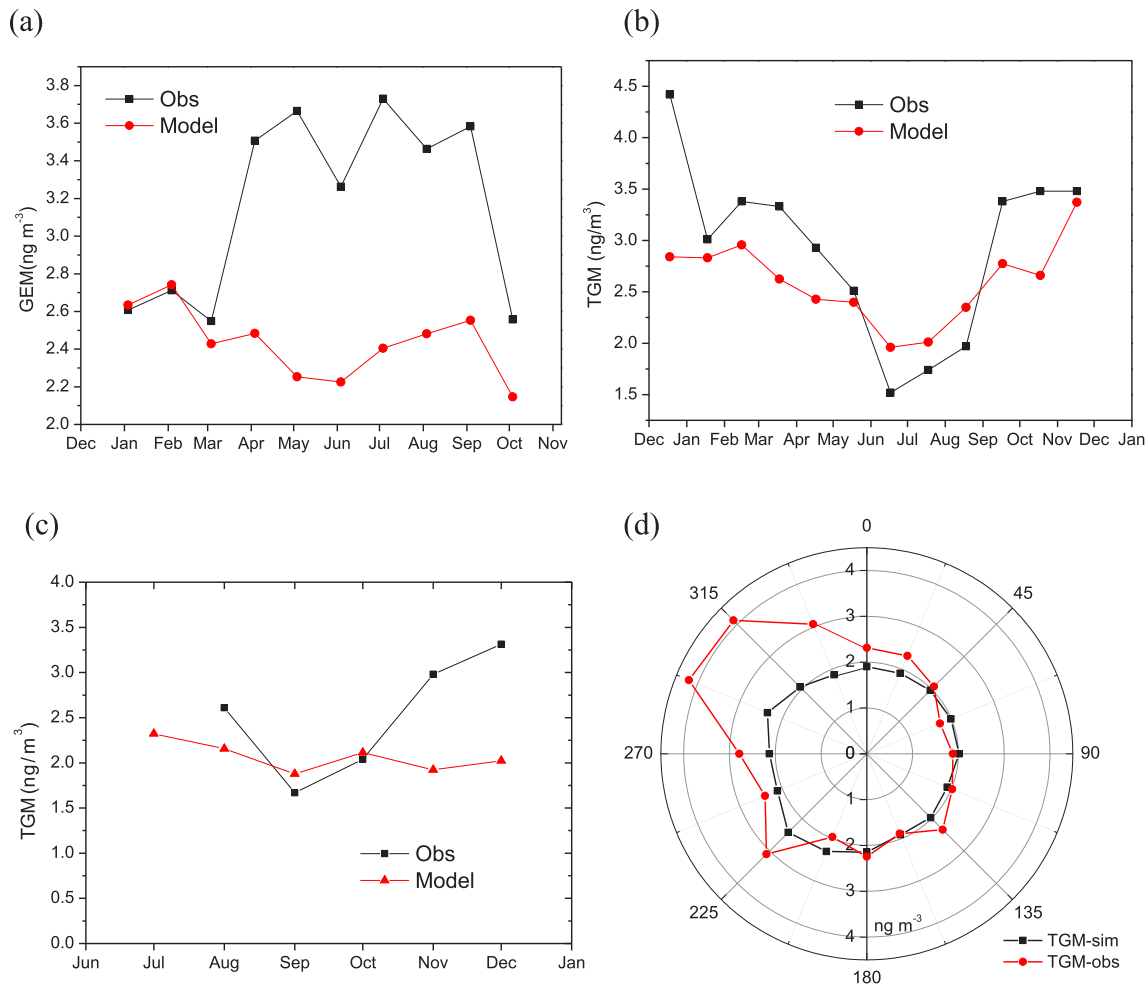


**Fig. 5.** Comparison of model predicted monthly total gaseous mercury (TGM) or Gaseous elemental mercury (GEM) concentrations with observations: (a) GEM (Miyun, 2009.1–2009.10); (b) TGM (Mt. Leigong, 2009.1–2009.12); (c) TGM (Chongming, 2009.8–2009.12); (d) Comparisons of modeled and observed TGM in different wind directions in Chongming Station (2009.9–2009.12).

The observation data for mercury deposition is quite limited and the reliability of available data should be further checked especially for dry deposition. Table 2 showed the comparisons of mercury wet deposition in 7 sites reported by literature and the GEOS-Chem model. The modeled wet deposition fluxes are 2–10 times higher than the observations in Mt. Gongga, Mt. Changbai, Mt. Leigong, Nam Co and Wujiang River Basin while the predicted precipitations are within an absolute bias of 35% for all these sites. In Tieshanping, the model result is consistent with the observations but the model overestimate the mercury content in rainfall because of the significant underestimation of precipitation (49%). General overestimation of RGM and PHg (see Table 1) might be the reason as both wet and dry deposition of mercury are mainly in the divalent or particulate form.

In conclusion, the GEOS-Chem model does well in reproducing the annual mercury concentrations in background sites, but underestimate the GEM or TGM in the rural sites by about 25–45%. The model generally overestimated RGM and PHg by a factor 2-5 but the absolute bias is not large. The overestimate of RGM and PHg might be the reason for overestimate of mercury deposition. In this study, we use the modeled annual average mercury concentrations and total deposition for comparison between different scenarios in a regional scale. Because of the consistency of background simulation results that signify the long range transport, great influence of local/regional sources to polluted regions as we can see in Table 2, and no great reduction of surface THg concentrations and deposition while shutting chemical modules in the model, the main factor for uncertainties of THg concentrations and depositions in industrial areas is mercury emission. Influence of this factor is significant for the absolute results but the ratio of different anthropogenic sources to total emissions are more important for relative differences of scenarios in this study. As we have incorporated latest results regarding mercury emission compilation, this model is suitable for further analysis at the current level of our understanding of mercury.

### *3.2. Contributions of typical industrial sources to THg concentration and deposition*

From the results of NAT scenario shown in Table 3, we can quantify the effects of mercury emissions from anthropogenic sources. In the study domain, the Hg emissions from natural and anthropogenic sources were 966.5t and 954.9t respectively. The anthropogenic emissions contributed 37.0% (341.9t) of the total deposition and 21.0% (0.4 ng $m^{-3}$) of the THg concentrations in the CHINA domain. In the NC, YRD and CC regions, the mercury deposition are 60% lower than that of the BASE scenario and the THg concentrations are more than 40% lower, which shows that

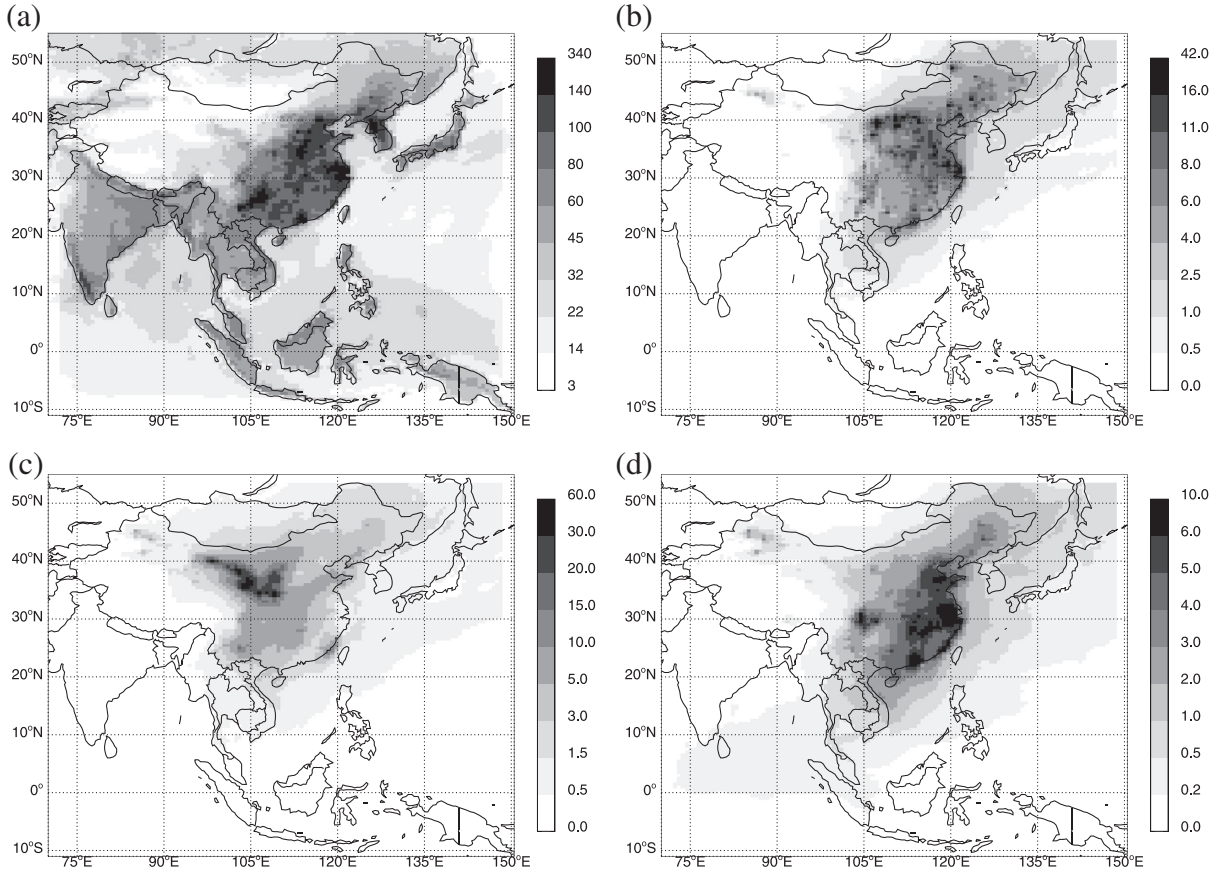


**Fig. 6.** (a) Model-predicted total mercury (THg) deposition, μg $m^{-2}$ $yr^{-1}$; (b) Difference of THg deposition between the NOPP scenario and BASE scenario, %; (c) Difference of THg deposition between the NONF scenario and BASE scenario, %; (d) Difference of THg deposition between the NOCE scenario and BASE scenario, %.

anthropogenic emissions have significant impacts in these domains.

As shown in Figs. 6b and 7b, shutting down the emission from power plants obviously decreased the THg concentration and deposition in East China. The total Hg emissions from coal-fired power plants (CFPPs) in China were 123.3 t, of which 14.9% (18.3 t), 35.5% (43.8 t) and 4.9% (6.0t) were from the YRD, NC and PRD, respectively. In the YRD, CFPPs contributed 25.0% of the total anthropogenic emissions, and contributed 10.8% (0.37 ng $m^{-3}$) of the THg concentrations, 13.3% (2.0 t) of the dry deposition and 9.1% (1.1 t) of the wet deposition. Around the city center of Nanjing and Shanghai, there were about 20%, 20% and 15% decline in THg concentrations, dry deposition and wet deposition, respectively. The large number and respective capacity of power plants in these areas resulted in a high emission intensification of 2 t $grid^{-1}$ $yr^{-1}$. In the NC domain, there was an 8.9% (0.28 ng $m^{-3}$) decline in THg concentrations, 10.3% (5.5 t) decline in dry deposition and 7.9% (2.4 t) in wet deposition. In Inner Mongol and Ningxia Province, there are large power plants with capacities larger than 1000 MW; the coal consumed in the two provinces is higher than average, and the mercury emissions by an individual plant is more than 1 t $yr^{-1}$. In the PRD, power plants contributed 23.2% to the anthropogenic mercury emissions while providing 7.1% (0.20 ng $m^{-3}$) to the THg concentrations and 8.0% (1.7 t) to the total deposition.

**Table 2**
Comparisons of model-predicted total mercury (THg) deposition in the BASE scenario with observations.

| Station | Period | Observations | | | Model | | | Reference |
|---|---|---|---|---|---|---|---|---|
| | | Wet deposition μg $m^{-2}$ $yr^{-1}$ | Rainfall mm | Dry deposition μg $m^{-2}$ $yr^{-1}$ | Wet deposition μg $m^{-2}$ $yr^{-1}$ | Rainfall mm | Dry deposition μg $m^{-2}$ $yr^{-1}$ | |
| Changchun, Jilin Province | July-99–July-00 | 63.7 | | 38.7 | 39.5 | | 65.2 | Fang et al. (2004) |
| Mt. Gongga, Sichuan Province | May-05–Apr-07 | 26.1 | | | 69.0 | 2906 | | Fu et al. (2010c) |
| Mt. Changbai, Jilin Province | Aug-05–Jul-06 | 8.4 | 630 | 16.5* | 26.7 | 760 | 30.1 | Wan et al. (2009a) |
| Mt. Leigong, Guizhou Province | May-08–May-09 | 6.1 | 1533 | | 71.3 | 1725 | | Fu et al. (2010a) |
| Mt. Leigong, Guizhou Province | Mar-05–Mar-06 | 16.8 | 1341 | | 71.3 | 1725 | | Wang et al. (2009) |
| Tieshangpin, Chongqing | Mar-05–Mar-06 | 29.0 | 1403 | | 28.1 | 720 | | Wang et al. (2009) |
| Nam Co, Tibet | Jul-10–Jul-11 | 1.8 | 365 | | 8.3 | 321 | | Huang et al. (2012) |
| Wujiang River Basin, Guizhou Province | 2006 | 34.7 | 963 | | 125.9 | 1292 | | Guo et al. (2008) |

Asterisk denotes the dry deposition in Mt. Changbai was determined by the difference of total Hg in through fall and rainwater, and the result above in Changchun City was not directly measured but estimated based on constant average deposition velocities of 0.01 cm $s^{-1}$ for GEM, 0.25 cm $s^{-1}$ for RGM and 0.5 cm $s^{-1}$ for PHg.

**Table 3**
Contributions of different sources to mercury concentrations and depositions, %.

| Sources | Region | NC | YRD | CC | PRD | SWC | China |
|---|---|---|---|---|---|---|---|
| (Base-NAT)/Base | THg | 46.9 | 50.4 | 44.9 | 38.5 | 37.4 | 21.0 |
| | Dry deposition | 66.5 | 72.5 | 59.3 | 56.1 | 52.7 | 37.5 |
| | Wet deposition | 69.0 | 69.3 | 67.0 | 55.9 | 66.5 | 36.5 |
| (Base-NOPP)/Base | THg | 8.9 | 10.8 | 7.0 | 7.1 | 4.5 | 2.3 |
| | Dry deposition | 10.3 | 13.3 | 8.3 | 9.4 | 5.2 | 4.1 |
| | Wet deposition | 7.9 | 9.1 | 6.8 | 6.4 | 4.5 | 2.9 |
| (Base-NONF)/Base | THg | 7.1 | 2.1 | 6.7 | 3.2 | 6.4 | 2.2 |
| | Dry deposition | 7.0 | 1.6 | 6.2 | 3.3 | 7.5 | 3.3 |
| | Wet deposition | 6.2 | 1.5 | 5.0 | 2.2 | 7.1 | 2.7 |
| (Base-NOCE)/Base | THg | 5.0 | 8.4 | 6.3 | 6.7 | 3.7 | 1.7 |
| | Dry deposition | 4.3 | 7.4 | 5.6 | 6.6 | 3.4 | 2.3 |
| | Wet deposition | 3.4 | 5.0 | 4.5 | 4.8 | 2.8 | 1.7 |

Notes: NC (North China), YRD (Yangtze River Delta), CC (Central China), PRD (Pearl River Delta), SWC (Southwest China) and CHINA (Chinese Mainland) are domains described in Section 3.1 and plotted in Fig. 3. Base, NAT, NOPP, NONF and NOCE are different scenarios. Base scenario was simulated with all anthropogenic and natural sources, NAT scenario with only natural sources, NOPP scenarios exclude emissions from coal-fired power plants, NONF scenarios exclude emissions from non-ferrous smelters, NOCE scenarios exclude emissions from cement plants.

Figs. 6c and 7c show the relative difference between NONF scenario and BASE scenario. In the CHINA domain, non-ferrous metal smelters contributed 2.2% (0.05 ng $m^{-3}$) of the THg concentrations, 3.3% (15.6 t) of the total dry deposition and 2.7% (12.2 t) of the total wet deposition. The effects of emissions from non-ferrous metal smelters were much greater in Gansu Province and Shaanxi Province because these provinces are the two largest emitters in China with high mercury concentrations in zinc ore and a large proportion of small scale plants with poor air pollution control devices (Wu et al., 2012). The contribution of non-ferrous metal smelters to THg concentrations are 11.2% (0.24 ng $m^{-3}$) and 17.2% (0.51 ng $m^{-3}$) while the contributions to the total deposition are 18.5% (2.1 t) and 20.2% (2.3 t) in Gansu and Shaanxi Province. In and around Lanzhou and Xi'an city, the capital of the two provinces, the impacts to THg concentrations are as high as 40–60% (1.2–2.8 ng $m^{-3}$) and the impacts to total deposition reached 30–50% (0.10–0.15 t). Table 3 shows the relative difference of mercury pollution between the NONF scenario and the BASE scenario in the five selected domains. In the domains of CC, NC and SWC, the non-ferrous metal smelters emitted 19.3% (10.2 t), 16.1% (33.3 t) and 18.9% (12.9 t) of total anthropogenic emissions and contributed 5–7% to the THg deposition and concentrations. In Henan Province of NC the contributions of non-ferrous smelters to THg concentrations reached 9.3% (0.4 ng $m^{-3}$). Near Kunming, the capital city of Yunnan Province, the contribution to total deposition was more than 10% (0.06–0.15 t).

Cement plants are also important mercury emitters. They contributed 13.7% of total anthropogenic emission in China. Figs. 6d and 7d show the relative difference between the NOCE scenario and the BASE scenario. Cement plants contributed 1.7% (0.04 ng $m^{-3}$) to the atmospheric THg, 2.3% (10.9 t) to the dry

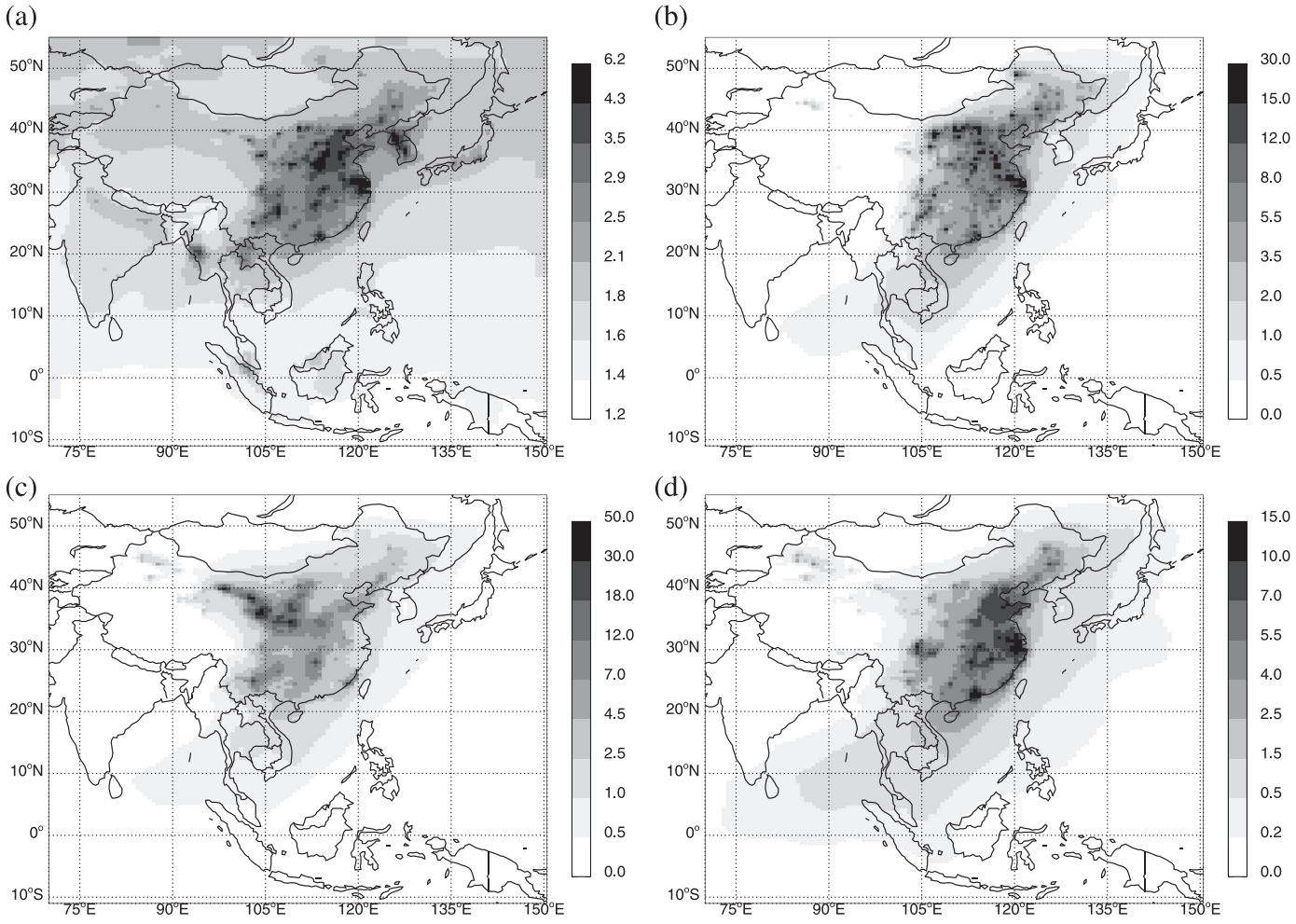


**Fig. 7.** (a) Model-predicted annual mean total mercury (THg) in surface layer, ng $m^{-3}$; (b) Difference of THg concentrations between the NOPP scenario and Base scenario, %; (c) Difference of THg concentrations between the NONF scenario and Base scenario, %; (d) Difference of THg concentrations between the NOCE scenario and Base scenario, %.

deposition and 1.7% (7.7 t) to the wet deposition in the CHINA domain. The influence was more evenly distributed over East China compared to power plants and non-ferrous metal smelters. Shandong Province, Henan Province and Hebei Province of the NC, Jiangsu Province and Zhejiang Province of the YRD, and Guangdong Province of the PRD are the six top emitters with an emission intensification of 3 times the national average, Hunan Province and Hubei Province of CC are also important emitters. The THg concentrations decreased by 5% in East China and Sichuan Province but the decline of wet deposition was shaper in the CC, PRD and YRD. In the PRD, the decline of THg concentrations, dry deposition and wet deposition were 6.7% (0.19 ng $m^{-3}$), 6.6% (0.7 t) and 4.8% (0.5 t) respectively while those in the YRD are 8.4% (0.29 ng $m^{-3}$), 7.4% (1.1 t) and 5.0% (0.6 t).

### 3.3. Implications for mercury emission control

Population exposure is one of the most important issues to be considered when mercury pollution control measures are taken. In China, rice and vegetation are the most important pathways because fish have short lifetimes (Li et al., 2012; Liu et al., 2012). Deposition of mercury to ecological system and subsequent methylation to more poisonous MeHg will be the main concern. Therefore total deposition is the most important factor for mercury control in terms of population exposure.

The regions with total mercury deposition over 150 μg $m^{-2}$ $yr^{-1}$ (0.5–0.7 t $grid^{-1}$) include the YRD, the PRD, the area connecting Guizhou Province and Yunnan Province in the SWC, and the north of Henan Province in the NC. These regions should be the priority of mercury pollution control areas.

On a sector level, the priority varies for the selected domains. For the NC, YRD and PRD, power plants should be first controlled. Presently, the installation of FGD and SCR increase rapidly and there will be about a 40–50% reduction in mercury emissions in the near future which will reduce the Hg deposition by about 4.0 t, 1.5 t and 2.0 t in these domains. For further reduction, other sectors should be considered. In the YRD and PRD, cement production should be the second priority of mercury control. The deposition will reduce about 0.7 t and 0.5 t if emissions from these two domains reduce by 40%. In Henan Province of the NC region, non-ferrous metal smelters, especially lead smelters are important emitters. Control of lead smelters in Henan Province will reduce 0.9t of the Hg deposition. The priority in Yunnan Province, Guizhou Province, Gansu Province and Shaanxi Province are zinc smelters which provide 0.4 t, 0.8 t, 1.9 t and 1.9 t of the Hg deposition respectively. Copper smelters are also important mercury sources in Yunnan Province.

In the Inner Mongol, Ningxia Province, the YRD and PRD regions, there are several large power plants which cause significant local impacts (20% THg and 15% total mercury deposition). Advanced control techniques such as activated carbon injection and bromine injection should be considered. For non-ferrous metal smelters, closing of small plants and requiring the installation of mercury reclaiming towers are effective ways to control mercury emissions.

## 4. Conclusions

In this study, the impacts of typical industrial sources in China were investigated using the GEOS-Chem East Asia nested model with updated mercury emission inventory in 2007. The model results were compared with observation data. Generally the model produces good performance on annual THg concentrations in background sites but underestimates it in rural sites. The model overestimates RGM and PHg by a factor of 2–5 which also results in the similar overestimation of mercury deposition.

The results showed that the anthropogenic emissions contributed 21% of THg concentrations and about 40% of total deposition in the Chinese mainland. In some areas of East China with large populations and developed economies, the contribution of anthropogenic emissions was 35–50% for THg concentrations and 50–70% for total deposition. Power plants are the most important emission sources in most areas of China, including the North China, YRD and PRD, which contributed 10.8% and 13.3% to THg and dry deposition in the YRD, 8.9% and 10.3% to THg and dry deposition in North China. The contribution of non-ferrous metal smelters is most significant in the Southwest China. 7.5% and 7.1% of wet depositions and dry depositions in SWC come from non-ferrous metal smelters. In the YRD, PRD and Central China, cement plants are also significant sources of mercury pollution. In the YRD, cement plants also increased THg and dry deposition by 8.4% and 7.4%, respectively.

This study first quantified the environmental impacts of anthropogenic mercury emission in China. To further understand the impacts of control measures, the atmospheric mercury emissions and chemistry should be improved and the uncertainty of model simulations shall be reduced.

## Acknowledgments

This work was funded by the Major State Basic Research Development Program of China (973 program) (Nos. 2013CB430001 & 2013CB430003), National Natural Science Foundation of China (No. 20 937 002) and China Scholarship Council (No. 201308110058). The corresponding author was also supported by the Program for New Century Excellent Talents in University (NCET-10-0532).

## References

AMAP/UNEP, 2013. Technical Background Report for the Global Mercury Assessment 2013. Arctic Monitoring and Assessment Programme, Oslo. Norway/UNEP Chemicals Branch, Geneva, Switzerland p. vi + 263.

Bullock, O.R., Atkinson, D., Braverman, T., Civerolo, K., Dastoor, A., Davignon, D., Ku, J.Y., Lohman, K., Myers, T.C., Park, R.J., Seigneur, C., Selin, N.E., Sistla, G., Vijayaraghavan, K., 2008. The North American Mercury Model Intercomparison Study (NAMMIS): study description and model-to-model comparisons. J. Geophys. Res.-Atmos. 113.

Bullock, O.R., Atkinson, D., Braverman, T., Civerolo, K., Dastoor, A., Davignon, D., Ku, J.Y., Lohman, K., Myers, T.C., Park, R.J., Seigneur, C., Selin, N.E., Sistla, G., Vijayaraghavan, K., 2009. An analysis of simulated wet deposition of mercury from the North American Mercury Model Intercomparison Study. J. Geophys. Res.-Atmos. 114.

Bullock, O.R., Brehme, K.A., 2002. Atmospheric mercury simulation using the CMAQ model: formulation description and analysis of wet deposition results. Atmos. Environ. 36, 2135–2146.

Chand, D., Jaffe, D., Prestbo, E., Swartzendruber, P.C., Hafner, W., Weiss-Penzias, P., Kato, S., Takami, A., Hatakeyama, S., Kajii, Y., 2008. Reactive and particulate mercury in the Asian marine boundary layer. Atmos. Environ. 42, 7988–7996.

Chen, D., Wang, Y., McElroy, M.B., He, K., Yantosca, R.M., Le Sager, P., 2009. Regional CO pollution and export in China simulated by the high-resolution nested-grid GEOS-Chem model. Atmos. Chem. Phys. 9, 3825–3839.

Ci, Z.J., Zhang, X.S., Wang, Z.W., Niu, Z.C., 2011a. Atmospheric gaseous elemental mercury (GEM) over a coastal/rural site downwind of East China: temporal variation and long-range transport. Atmos. Environ. 45, 2480–2487.

Ci, Z.J., Zhang, X.S., Wang, Z.W., Niu, Z.C., Diao, X.Y., Wang, S.W., 2011b. Distribution and air-sea exchange of mercury (Hg) in the Yellow Sea. Atmos. Chem. Phys. 11, 2881–2892.

Dou, H.Y., 2012. Characteristics of Speciated Atmospheric Mercury Concentrations at a Rural Site of Yangtze Delta, China. School of Environment. Tsinghua University, Beijing.

Fang, F.M., Wang, Q.C., Li, J.F., 2004. Urban environmental mercury in Changchun, a metropolitan city in Northeastern China: source, cycle, and fate. Sci. Total Environ. 330, 159–170.

Fu, X., Wang, S.X., Zhao, B., Xing, J., Cheng, Z., Liu, H., Hao, J.M., 2013. Emission inventory of primary pollutants and chemical speciation in 2010 for the Yangtze River Delta region, China. Atmos. Environ. 70, 39–50.

Fu, X.W., Feng, X., Dong, Z.Q., Yin, R.S., Wang, J.X., Yang, Z.R., Zhang, H., 2010a. Atmospheric gaseous elemental mercury (GEM) concentrations and mercury

depositions at a high-altitude mountain peak in south China. Atmos. Chem. Phys. 10, 2425–2437.
Fu, X.W., Feng, X., Liang, P., Deliger, Zhang, H., Ji, J., Liu, P., 2012a. Temporal trend and sources of speciated atmospheric mercury at Waliguan GAW station, Northwestern China. Atmos. Chem. Phys. 12, 1951–1964.
Fu, X.W., Feng, X., Shang, L.H., Wang, S.F., Zhang, H., 2012b. Two years of measurements of atmospheric total gaseous mercury (TGM) at a remote site in Mt. Changbai area, Northeastern China. Atmos. Chem. Phys. 12, 4215–4226.
Fu, X.W., Feng, X.B., Zhang, G., Xu, W.H., Li, X.D., Yao, H., Liang, P., Li, J., Sommar, J., Yin, R.S., Liu, N., 2010b. Mercury in the marine boundary layer and seawater of the South China Sea: concentrations, sea/air flux, and implication for land outflow. J. Geophys. Res.-Atmos. 115.
Fu, X.W., Feng, X.B., Zhu, W.Z., Rothenberg, S., Yao, H., Zhang, H., 2010c. Elevated atmospheric deposition and dynamics of mercury in a remote upland forest of southwestern China. Environ. Pollut. 158, 2324–2333.
Fu, X.W., Feng, X.B., Zhu, W.Z., Wang, S.F., Lu, J.L., 2008a. Total gaseous mercury concentrations in ambient air in the eastern slope of Mt. Gongga, South-Eastern fringe of the Tibetan plateau, China. Atmos. Environ. 42, 970–979.
Fu, X.W., Feng, X.B., Zhu, W.Z., Zheng, W., Wang, S.F., Lu, J.Y., 2008b. Total particulate and reactive gaseous mercury in ambient air on the eastern slope of the Mt. Gongga area, China. Appl. Geochem. 23, 408–418.
Gbor, P.K., Wen, D.Y., Meng, F., Yang, F.Q., Zhang, B.N., Sloan, J.J., 2006. Improved model for mercury emission, transport and deposition. Atmos. Environ. 40, 973–983.
Guo, Y.N., Feng, X.B., Li, Z.G., He, T.R., Yan, H.Y., Meng, B., Zhang, J.F., Qiu, G.L., 2008. Distribution and wet deposition fluxes of total and methyl mercury in Wujiang River Basin, Guizhou, China. Atmos. Environ. 42, 7096–7103.
Holmes, C.D., Jacob, D.J., Corbitt, E.S., Mao, J., Yang, X., Talbot, R., Slemr, F., 2010. Global atmospheric model for mercury including oxidation by bromine atoms. Atmos. Chem. Phys. 10, 12037–12057.
Huang, J., Kang, S.C., Zhang, Q.G., Yan, H.Y., Guo, J.M., Jenkins, M.G., Zhang, G.S., Wang, K., 2012. Wet deposition of mercury at a remote site in the Tibetan Plateau: concentrations, speciation, and fluxes. Atmos. Environ. 62, 540–550.
Kim, K.H., Kim, M.Y., Kim, J., Lee, G., 2002. The concentrations and fluxes of total gaseous mercury in a western coastal area of Korea during late March 2001. Atmos. Environ. 36, 3413–3427.
Kuo, T.H., Chang, C.F., Urba, A., Kvietkus, K., 2006. Atmospheric gaseous mercury in northern Taiwan. Sci. Total Environ. 368, 10–18.
Li, P., Feng, X.B., Yuan, X.B., Chan, H.M., Qiu, G.L., Sun, G.X., Zhu, Y.G., 2012. Rice consumption contributes to low level methylmercury exposure in southern China. Environ. Int. 49, 18–23.
Li, Z., Xia, C.H., Wang, X.M., Xiang, Y.R., Xie, Z.Q., 2011. Total gaseous mercury in Pearl River Delta region, China during 2008 winter period. Atmos. Environ. 45, 834–838.
Lin, C.J., Pan, L., Streets, D.G., Shetty, S.K., Jang, C., Feng, X., Chu, H.W., Ho, T.C., 2010. Estimating mercury emission outflow from East Asia using CMAQ-Hg. Atmos. Chem. Phys. 10, 1853–1864.
Lin, C.J., Pongprueks, P., Rusell Bulock, O., Lindberg, S.E., Pehkonen, S.O., Jang, C., Braverman, T., Ho, T.C., 2007. Scientific uncertainties in atmospheric mercury models II: sensitivity analysis in the CONUS domain. Atmos. Environ. 41, 6544–6560.
Lin, C.J., Pongprueksa, P., Lindberg, S.E., Pehkonen, S.O., Byun, D., Jang, C., 2006. Scientific uncertainties in atmospheric mercury models I: model science evaluation. Atmos. Environ. 40, 2911–2928.
Liu, B., Yan, H.Y., Wang, C.P., Li, Q.H., Guedron, S., Spangenberg, J.E., Feng, X.B., Dominik, J., 2012. Insights into low fish mercury bioaccumulation in a mercury-contaminated reservoir, Guizhou, China. Environ. Pollut. 160, 109–117.
Liu, N., Qiu, G.G., Landis, M.S., Feng, X.B., Fu, X.W., Shang, L.H., 2011. Atmospheric mercury species measured in Guiyang, Guizhou province, southwest China. Atmos. Res. 100, 93–102.
Lohman, K., Seigneur, C., Edgerton, E., Jansen, J., 2006. Modeling mercury in power plant plumes. Environ. Sci. Technol. 40, 3848–3854.
Nguyen, H.T., Kim, K.H., Kim, M.Y., Hong, S.M., Youn, Y.H., Shon, Z.H., Lee, J.S., 2007. Monitoring of atmospheric mercury at a global atmospheric watch (GAW) site on An-Myun Island, Korea. Water Air Soil. Pollut. 185, 149–164.
Pan, L., Lin, C.J., Carmichael, G.R., Streets, D.G., Tang, Y.H., Woo, J.H., Shetty, S.K., Chu, H.W., Ho, T.C., Friedli, H.R., Feng, X.B., 2010. Study of atmospheric mercury budget in East Asia using STEM-Hg modeling system. Sci. Total Environ. 408, 3277–3291.
Pongprueksa, P., Lin, C.J., Lindberg, S.E., Jang, C., Braverman, T., Bullock, O.R., Ho, T.C., Chu, H.W., 2008. Scientific uncertainties in atmospheric mercury models III: boundary and initial conditions, model grid resolution, and Hg(II) reduction mechanism. Atmos. Environ. 42, 1828–1845.
Ryaboshapko, A., Bullock, O.R., Christensen, J., Cohen, M., Dastoor, A., Ilyin, I., Petersen, G., Syrakov, D., Artz, R.S., Davignon, D., Draxler, R.R., Munthe, J., 2007a. Intercomparison study of atmospheric mercury models: 1. Comparison of models with short-term measurements. Sci. Total Environ. 376, 228–240.
Ryaboshapko, A., Bullock, O.R., Christensen, J., Cohen, M., Dastoor, A., Ilyin, I., Petersen, G., Syrakov, D., Travnikov, O., Artz, R.S., Davignon, D., Draxler, R.R., Munthe, J., Pacyna, J., 2007b. Intercomparison study of atmospheric mercury models: 2. Modelling results vs. long-term observations and comparison of country deposition budgets. Sci. Total Environ. 377, 319–333.
Selin, N.E., Jacob, D.J., 2008. Seasonal and spatial patterns of mercury wet deposition in the United States: constraints on the contribution from North American anthropogenic sources. Atmos. Environ. 42, 5193–5204.
Selin, N.E., Jacob, D.J., Park, R.J., Yantosca, R.M., Strode, S., Jaegle, L., Jaffe, D., 2007. Chemical cycling and deposition of atmospheric mercury: global constraints from observations. J. Geophys. Res.-Atmos. 112.
Slemr, F., Brunke, E.G., Ebinghaus, R., Kuss, J., 2011. Worldwide trend of atmospheric mercury since 1995. Atmos. Chem. Phys. 11, 4779–4787.
Slemr, F., Brunke, E.G., Ebinghaus, R., Temme, C., Munthe, J., Wangberg, I., Schroeder, W., Steffen, A., Berg, T., 2003. Worldwide trend of atmospheric mercury since 1977. Geophys. Res. Lett. 30.
Streets, D.G., Hao, J.M., Wu, Y., Jiang, J.K., Chan, M., Tian, H.Z., Feng, X.B., 2005. Anthropogenic mercury emissions in China. Atmos. Environ. 39, 7789–7806.
Streets, D.G., Zhang, Q., Wu, Y., 2009. Projections of global mercury emissions in 2050. Environ. Sci. Technol. 43, 2983–2988.
Strode, S.A., Jaegle, L., Jaffe, D.A., Swartzendruber, P.C., Selin, N.E., Holmes, C., Yantosca, R.M., 2008. Trans-Pacific transport of mercury. J. Geophys. Res.-Atmos. 113.
Wan, Q., Feng, X.B., Lu, J., Zheng, W., Song, X.J., Li, P., Han, S.J., Xu, H., 2009a. Atmospheric mercury in Changbai Mountain area, northeastern China II. The distribution of reactive gaseous mercury and particulate mercury and mercury deposition fluxes. Environ. Res. 109, 721–727.
Wan, Q., Feng, X.B., Lu, J.L., Zheng, W., Song, X.J., Han, S.J., Xu, H., 2009b. Atmospheric mercury in Changbai Mountain area, northeastern China I. The seasonal distribution pattern of total gaseous mercury and its potential sources. Environ. Res. 109, 201–206.
Wang, S.X., Song, J.X., Li, G.H., Wu, Y., Zhang, L., Wan, Q., Streets, D.G., Chin, C.K., Hao, J.M., 2010a. Estimating mercury emissions from a zinc smelter in relation to China's mercury control policies. Environ. Pollut. 158, 3347–3353.
Wang, S.X., Zhang, L., Li, G.H., Wu, Y., Hao, J.M., Pirrone, N., Sprovieri, F., Ancora, M.P., 2010b. Mercury emission and speciation of coal-fired power plants in China. Atmos. Chem. Phys. 10, 1183–1192.
Wang, S.X., Zhang, L., Wu, Y., Ancora, M.P., Zhao, Y., Hao, J.M., 2010c. Synergistic mercury removal by Conventional Pollutant control Strategies for coal-fired power plants in China. J. Air Waste Manag. Assoc. 60, 722–730.
Wang, T.J., Zhu, J.L., Wang, T.T., 2013. Numerical study on atmospheric mercury over China. China Sciencepaper Online. http://www.paper.edu.cn/releasepaper/content/201302-499.
Wang, Y.X., McElroy, M.B., Jacob, D.J., Yantosca, R.M., 2004. A nested grid formulation for chemical transport over Asia: applications to CO. J. Geophys. Res.-Atmos. 109.
Wang, Z.W., Chen, Z.S., Duan, N., Zhang, X.S., 2007. Gaseous elemental mercury concentration in atmosphere at urban and remote sites in China. J. Environ. Sci.-China 19, 176–180.
Wang, Z.W., Zhang, X.S., Xiao, J.S., Zhijia, C., Yu, P.Z., 2009. Mercury fluxes and pools in three subtropical forested catchments, southwest China. Environ. Pollut. 157, 801–808.
Wu, Q.R., Wang, S.X., Zhang, L., Song, J.X., Yang, H., Meng, Y., 2012. Update of mercury emissions from China's primary zinc, lead and copper smelters, 2000-2010. Atmos. Chem. Phys. 12, 11153–11163.
Wu, Y., Wang, S.X., Streets, D.G., Hao, J.M., Chan, M., Jiang, J.K., 2006. Trends in anthropogenic mercury emissions in China from 1995 to 2003. Environ. Sci. Technol. 40, 5312–5318.
Zhang, H., 2011. Concentrations of Speciated Atmospheric Mercury a High-altitude Background station in the Shangri-La area of Tibetan Plateau, China. In: 10th International Conference on Mercury as a Global Pollutant. Halifax, Canada.
Zhang, L., Wang, S.X., Wang, L., Hao, J.M., 2013. Atmospheric mercury concentration and chemical speciation at a rural site in Beijing, China: implication of mercury emission sources. Atmos. Chem. Phys. Discuss. 12, 12177–12211.
Zhang, Y., Jaegle, L., van Donkelaar, A., Martin, R.V., Holmes, C.D., Amos, H.M., Wang, Q., Talbot, R., Artz, R., Brooks, S., Luke, W., Holsen, T.M., Felton, D., Miller, E.K., Perry, K.D., Schmeltz, D., Steffen, A., Tordon, R., Weiss-Penzias, P., Zsolway, R., 2012. Nested-grid simulation of mercury over North America. Atmos. Chem. Phys. 12, 6095–6111.